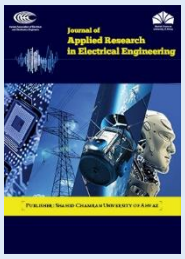
Shahid Chamran University of Ahvaz

Iranian Association of Electrical and Electronics Engineers

Journal of Applied Research in Electrical Engineering

E-ISSN: 2783-2864
P-ISSN: 2717-414X
Homepage: https://jaree.scu.ac.ir/



Research Article

On the Radiation from Infinite Length Lossless Two Wire Transmission Lines

Farhad Mazlumi [1,*]

[1] *Aeronautical Telecommunications Department, Civil Aviation Technology College, MehrAbad International Airport, Tehran, Iran*

* *Corresponding Author: mazlumi@catc.ac.ir*

Abstract: The electromagnetic radiation characteristics of infinite length, lossless two-wire transmission lines are investigated in this paper. Through rigorous analytical calculations, the absence of radiation perpendicular to the wire length in such configurations is demonstrated. The analysis reveals that Transverse Electromagnetic (TEM) wave propagation is exhibited in both single and parallel wire scenarios, with power flow confined exclusively along the wires. To support the analysis, the single-wire case is simulated using ANSYS HFSS, and the obtained results are compared with the derived analytical expressions. These findings are further validated through comparisons with established models, such as the coaxial cable and two-wire transmission lines with non-zero radius. A common misconception regarding radiation in ideal transmission line systems is clarified by this study, and a robust theoretical framework for understanding electromagnetic behavior in these structures is provided. The presented methodology offers a foundation for exploring more complex scenarios involving non-ideal transmission line configurations.

Keywords: Transmission line, Electromagnetic Radiation, Antennas, Transverse Electromagnetic (TEM).

Article history
Received 28 December 2024 ; Revised 13 April 2026 ; Accepted 23 September 2026 ; Published online 10 October 2026.
© 2026 Published by Shahid Chamran University of Ahvaz & Iranian Association of Electrical and Electronics Engineers (IAEEE)
How to cite this article
F Mazlumi, " On the radiation from infinite length lossless two wire transmission lines," *J. Appl. Res. Electr. Eng.*, vol. 4, no. 2, pp. 282-288, 2025.
DOI: https://doi.org/10.22055/jaree.2026.48634.1148

1. INTRODUCTION

The parallel two-wire configuration serves as a widely employed transmission line in educational contexts, often depicted as a representative example [1]. Its popularity stems from the relative simplicity of its sketch compared to other transmission line configurations. Moreover, it finds practical application in the transmission of power and telephone signals, making it a ubiquitous presence in various settings.

The exploration of radiation from transmission lines has intrigued researchers since the early years following the discovery of Maxwell's electromagnetic equations. Early scientists noted that infinite-length lossless transmission lines did not exhibit radiation. Carson's paper [2] specifically reports the conclusions reached by Mie [3] and MacDonald [4], who independently affirmed that an infinite-length, lossless two-wire transmission line does not emit radiation.

While this paper primarily focuses on lossless infinite-length transmission lines, it is valuable to explore relevant literature pertaining to lossy or finite-length transmission lines. Steinmetz's seminal work in 1919 [5] delves into the frequency-dependent variations of the transmission line constants—R, L, C, and G. His findings highlight the substantial increase in resistance and inductance at higher frequencies, attributed to the skin effect. Additionally, Steinmetz demonstrates that the capacitance of a line decreases at high frequencies due to the radiation of electromagnetic energy.

Carson's 1921 comprehensive theory addresses radiation from transmission lines of any length [2]. He establishes that the radiation is proportionate to the square of the current on the line, reaching its peak at resonance frequencies. Carson further illustrates how terminating a line in a matched load can mitigate radiation. Manneback's 1923 extension of Carson's theory incorporates the impact of losses on radiation from transmission lines [6]. He discerns that while losses can diminish radiation, they may also intensify it at specific frequencies.

Sinclair's 1948 contribution involves a theory for modelling electromagnetic systems, emphasizing the use of

infinite-length transmission lines to model radiation from antennas and other radiating structures [7]. Storer's 1951 calculations focus on the radiation resistance of a two-wire line [8]. He establishes that the radiation resistance is proportional to the square of the current, peaking at resonance frequencies. Storer also underscores the potential reduction of radiation resistance by terminating the two-wire line in a matched load.

Ianconescu and Vulfin [9] conduct a detailed investigation into the radiation emanating from two-conductor non-isolated TEM transmission lines with arbitrary cross-sections in free space. Their comprehensive analysis spans infinite, semi-infinite, and finite transmission lines with both matched and non-matched terminations. The results shed light on the fact that infinite transmission lines maintain a radiation-free characteristic, while a smooth and continuous transition is observed in the radiation patterns between finite and semi-infinite transmission lines. It is noteworthy that their analysis assumes an electrically small distance between leads, and they employ far field approximations for computational efficiency.

Tashiro et al. [10] present a novel transmission line model that integrates the effects of radiation reaction. Rooted in Sommerfeld's principal wave propagation, this model is specifically applicable to finite-length single-conductor transmission lines lacking a return current path. Notably, the model achieves a self-consistent representation by explicitly incorporating radiation reaction effects.

Dai and Bremer [11] extend the resistance matrix formulation for multi-conductor transmission lines including shields, modelling imperfect shielding via transfer impedance. While rigorous for shielded cables, this approach does not apply to an unshielded single conductor in free space. Liang et al. [12] combine the Baum–Liu–Tesche (BLT) model with the charge simulation method to analyze field coupling to transmission lines inside underground utility tunnels. Although this work accounts for field distortion due to surrounding structures, it assumes the presence of a tunnel and multiple conductors, again deviating from the canonical infinite single-wire problem. Tashiro et al. [13] present a single-conductor transmission-line model for bent wire structures comprising multiple straight elements. They use their presented model to predict the field emissions associated with the antenna mode around a bend.

Classical treatments of cylindrical wave excitation and related structures can be found in standard electromagnetic textbooks. For example, Harrington [14] discusses sources of cylindrical waves under the assumption of uniform excitation, while Balanis [15] analyzes radial waveguides based on finite parallel-plate configurations supporting standing-wave modes. Although these formulations provide important physical insights, they differ from the present problem in that they do not consider a position-dependent traveling-wave excitation along an unbounded single conductor in free space.

While the absence of radiation from an ideal, lossless, infinite-length two-conductor transmission line is well established in classical electromagnetic theory, a persistent misconception continues to appear among current students and even in some informal technical discussions. This misunderstanding typically stems from an oversimplified explanation that attributes the absence of radiation solely to the cancellation of opposing currents, without a full appreciation of the underlying field behavior. The present work re-examines this classical problem through exact analytical formulations, offering a rigorous, step-by-step derivation that confirms the established result while making the reasoning transparent and pedagogically accessible. By bridging the gap between historical literature and modern instructional needs, the study not only reaffirms a foundational electromagnetic principle but also enhances its clarity for contemporary education and practice.

Following this introduction, an exact radiation analysis is presented for two cases: a single wire and a pair of parallel wires, both of which are straight, lossless, and of infinite length. For each configuration, the derivation is carried out with careful attention to both the mathematical details and the physical interpretation of the results. The analytical results for the single-wire case are then validated through full-wave simulation using ANSYS HFSS. Subsequently, the analytical findings are compared with established models from the literature, including coaxial cables and two-wire transmission lines with non-zero radius, thereby highlighting their consistency while clarifying the origin of common misconceptions. The paper concludes with a summary of the main contributions and a discussion of the implications for electromagnetic theory education.

2. RADIATION FROM WIRE TRANSMISSION LINES

In this section, the analysis focuses on computing the radiation emanating from an infinitely long, lossless transmission line, considering two distinct cases. First, the radiation from a single thin wire is determined, and the results are then applied to compute the fields produced by two parallel wires. In both cases, the wires are assumed to be straight, situated in a free-space environment. The notations and formulations follow those presented in Ref [16], in which the electric and magnetic potentials are expressed in terms of the current flowing along the wires and the linear electric charge density distributed on them. From these potentials, the electric and magnetic fields are subsequently obtained. The calculations are exact, with no approximations applied at any stage of the derivations.

2.1. Single Wire

A single straight wire with infinite length and zero radius lying on z-axis in free space is assumed (Fig. 1). It carries a travelling wave current $I(z)$,

$$I(z) = I_0 \mathrm{e}^{-\mathrm{j}k_0 z} \tag{1}$$

where I_0 is the amplitude of the current and e is the base of the natural logarithm. The free-space wavenumber (k_0) is expressed in terms of the free-space and electric permittivity (ε_0) and magnetic permeability (μ_0) as follows

$$k_0 = \omega\sqrt{\mu_0 \varepsilon_0} \tag{2}$$

It is important to note that $I(z)$ in (1) is a phasor, and its time dependency is represented by $\mathrm{e}^{\mathrm{j}\omega t}$, where ω is the angular frequency and t is time.

Since the current $I(z)$ in (1) flows along the wire, the

continuity equation [16] requires the presence of a corresponding linear electric charge density ρ_l along the z-axis, given by

$$\rho_l(z) = -\frac{1}{\mathrm{j}\omega}\frac{\mathrm{d}I}{\mathrm{d}z} = \frac{k_0}{\omega} I_0 \mathrm{e}^{-\mathrm{j}k_0 z} \tag{3}$$

Expressed in terms of scalar electric potential (ϕ) and magnetic vector potential (**A**), the electric field intensity (**E**) takes the following form [16].

$$\mathbf{E} = -\nabla\phi - \mathrm{j}\omega\mathbf{A} \tag{4}$$

The magnetic and electric potentials can be determined in cylindrical coordinates based on the current and linear charge density, as outlined below. Since the current flows along a zero-radius wire, the volume integrals in the calculation of **A** and ϕ reduce to one-dimensional integrals over the z-coordinate.

$$\begin{aligned}\mathbf{A}(\mathbf{R}) &= \frac{\mu_0}{4\pi}\int_{-\infty}^{+\infty} \hat{\mathbf{z}} I(z') G(|\mathbf{R}-\mathbf{R}'|)\mathrm{d}z' \\ &= \frac{\mu_0}{4\pi}\int_{-\infty}^{+\infty} \left(\hat{\mathbf{z}} I_0 \mathrm{e}^{-\mathrm{j}k_0 z'}\right) G(|\mathbf{R}-\mathbf{R}'|)\mathrm{d}z' \\ &= \hat{\mathbf{z}}\frac{\mu_0}{4\pi} I_0 \int_{-\infty}^{+\infty} \mathrm{e}^{-\mathrm{j}k_0 z'} G(|\mathbf{R}-\mathbf{R}'|)\mathrm{d}z'\end{aligned} \tag{5}$$

$$\begin{aligned}\phi(\mathbf{R}) &= \frac{1}{4\pi\varepsilon_0}\int_{-\infty}^{+\infty} \rho_l(z') G(|\mathbf{R}-\mathbf{R}'|)\mathrm{d}z' \\ &= \frac{1}{4\pi\varepsilon_0}\int_{-\infty}^{+\infty} \left(\frac{k}{\omega} I_0 \mathrm{e}^{-\mathrm{j}k_0 z'}\right) G(|\mathbf{R}-\mathbf{R}'|)\mathrm{d}z' \\ &= \frac{\eta_0}{4\pi} I_0 \int_{-\infty}^{+\infty} \mathrm{e}^{-\mathrm{j}k_0 z'} G(|\mathbf{R}-\mathbf{R}'|)\mathrm{d}z'\end{aligned} \tag{6}$$

where G is

$$G(|\mathbf{R}-\mathbf{R}'|) = \frac{\mathrm{e}^{-\mathrm{j}k_0|\mathbf{R}-\mathbf{R}'|}}{|\mathbf{R}-\mathbf{R}'|} = \frac{\mathrm{e}^{-\mathrm{j}k_0\sqrt{(z-z')^2+r^2}}}{\sqrt{(z-z')^2+r^2}} = G(r,z,z') \tag{7}$$

In (5)-(7), η_0 ($=\sqrt{\mu_0/\varepsilon_0}$) is the free space intrinsic impedance, (r, φ, z) represents the coordinates of the observation point, and (r' = 0, φ' = 0, z') represents the coordinates of the source point on the wire. A hat symbol indicates a unit vector, while $|\cdot|$ denotes the magnitude of a vector. The vectors **R** and **R′** correspond to the position vectors of the observation and source points, respectively, i.e., $\mathbf{R} = r\hat{\mathbf{r}} + z\hat{\mathbf{z}}$ and $\mathbf{R}' = z'\hat{\mathbf{z}}$.

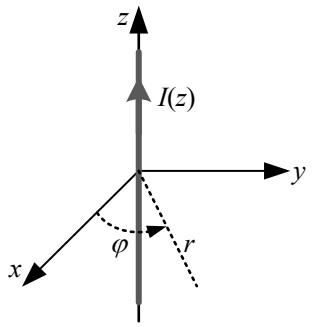


Fig. 1: A single straight wire with infinite length lying on z-axis.

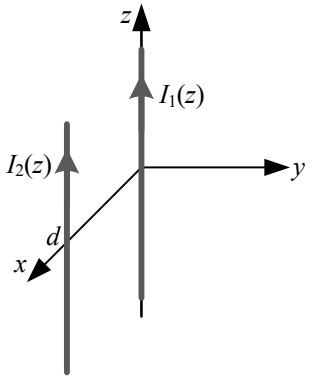


Fig. 2: Two infinitely long straight wires positioned parallel to the z-axis at a distance d.

To calculate the electric field intensity using (4), the gradient of the electric potential in (6) is to be obtained. To achieve this, the order of precedence of integral and gradient operators is changed and the gradient is calculated with respect to non-primed position variables. Subsequently, (4) can be written as follows

$$\begin{aligned}\mathbf{E}(\mathbf{R}) &= -\frac{\eta_0}{4\pi} I_0 \int_{-\infty}^{+\infty} \mathrm{e}^{-\mathrm{j}k_0 z'} \nabla G(r,z,z')\mathrm{d}z' \\ &\quad -\hat{\mathbf{z}}\mathrm{j}\omega\frac{\mu_0}{4\pi} I_0 \int_{-\infty}^{+\infty} \mathrm{e}^{-\mathrm{j}k_0 z'} G(r,z,z')\mathrm{d}z' \\ &= -\frac{\eta_0}{4\pi} I_0 \int_{-\infty}^{+\infty} \mathrm{e}^{-\mathrm{j}k_0 z'} \left(\hat{\mathbf{r}}\frac{\partial G}{\partial r} + \hat{\mathbf{z}}\frac{\partial G}{\partial z}\right)\mathrm{d}z' \\ &\quad -\hat{\mathbf{z}}\mathrm{j}\omega\frac{\mu_0}{4\pi} I_0 \int_{-\infty}^{+\infty} \mathrm{e}^{-\mathrm{j}k_0 z'} G\mathrm{d}z'\end{aligned} \tag{8}$$

To simplify the presentation and avoid lengthy formulas, the r- and z-components of the electric field are calculated separately. The calculations outlined below demonstrates that the z-component of the electric field intensity (E_z) in (8) is determined to be zero.

$$
\begin{aligned}
E_z(\mathbf{R}) &= -\frac{\eta_0}{4\pi} I_0 \int_{-\infty}^{+\infty} \mathrm{e}^{-\mathrm{j}k_0 z'} \left(\frac{\partial G}{\partial z} + \mathrm{j}\omega \frac{\mu_0}{\eta_0} G \right) \mathrm{d}z' \\
&= -\frac{\eta_0}{4\pi} I_0 \int_{-\infty}^{+\infty} \left(\mathrm{e}^{-\mathrm{j}k_0 z'} \frac{\partial G}{\partial z} + \mathrm{j}k_0 \mathrm{e}^{-\mathrm{j}k_0 z'} G \right) \mathrm{d}z' \\
&= -\frac{\eta_0}{4\pi} I_0 \int_{-\infty}^{+\infty} \left(-\mathrm{e}^{-\mathrm{j}k_0 z'} \frac{\partial G}{\partial z'} - G \frac{\partial \mathrm{e}^{-\mathrm{j}k_0 z'}}{\partial z'} \right) \mathrm{d}z' \\
&= \frac{\eta_0}{4\pi} I_0 \int_{-\infty}^{+\infty} \frac{\partial}{\partial z'} \left(\mathrm{e}^{-\mathrm{j}k_0 z'} G \right) \mathrm{d}z' \\
&= \frac{\eta_0}{4\pi} I_0 \left(\mathrm{e}^{-\mathrm{j}k_0 z'} \frac{\mathrm{e}^{-\mathrm{j}k_0 \sqrt{(z-z')^2 + r^2}}}{\sqrt{(z-z')^2 + r^2}} \right)_{z'=-\infty}^{z'=+\infty} = 0
\end{aligned}
\tag{9}
$$

It is noted that, in deriving the above result, the following relation was utilized:

$$
\frac{\partial G}{\partial z'} = -\frac{\partial G}{\partial z} \tag{10}
$$

Also, the r-component of the electric field intensity (E_r) in (8) is simplified and takes the following form

$$
\begin{aligned}
E_r &= -\frac{\eta_0}{4\pi} I_0 \int_{-\infty}^{+\infty} \mathrm{e}^{-\mathrm{j}k_0 z'} \frac{\partial}{\partial r} G(r, z, z') \mathrm{d}z' \\
&= -\frac{\eta_0}{4\pi} I_0 r \int_{-\infty}^{+\infty} \frac{\partial}{\partial z'} \left(\frac{\mathrm{e}^{-\mathrm{j}k_0 z'} G(r, z, z')}{\sqrt{(z-z')^2 + r^2} - (z-z')} \right) \mathrm{d}z' \\
&= -\frac{\eta_0}{4\pi} I_0 r \left(\frac{\mathrm{e}^{-\mathrm{j}k_0 z'} G(r, z, z')}{\sqrt{(z-z')^2 + r^2} - (z-z')} \right)_{z'=-\infty}^{z'=+\infty} \\
&= -\frac{\eta_0}{4\pi} I_0 r \left(-\frac{2}{r^2} \mathrm{e}^{-\mathrm{j}k_0 z} \right) = I_0 \frac{\eta_0}{2\pi r} \mathrm{e}^{-\mathrm{j}k_0 z}
\end{aligned}
\tag{11}
$$

It is noted that, in deriving the above equation, the following identity was employed:

$$
\mathrm{e}^{-\mathrm{j}k_0 z'} \frac{\partial G}{\partial r} = r \frac{\partial}{\partial z'} \left(\frac{\mathrm{e}^{-\mathrm{j}k_0 z'} G}{\sqrt{(z-z')^2 + r^2} - (z-z')} \right) \tag{12}
$$

Finally, the electric and magnetic fields around the single wire are

$$
\mathbf{E}(\mathbf{R}) = \hat{\mathbf{r}} I_0 \frac{\eta}{2\pi r} \mathrm{e}^{-\mathrm{j}k_0 z} = I_0 \frac{\eta \mathbf{r}}{2\pi r^2} \mathrm{e}^{-\mathrm{j}k_0 z} \tag{13}
$$

$$
\begin{aligned}
\mathbf{H}(\mathbf{R}) &= \frac{1}{\mu_0} \nabla \times \mathbf{A} \\
&= -\hat{\boldsymbol{\varphi}} \frac{I_0}{4\pi} \int_{-\infty}^{+\infty} \mathrm{e}^{-\mathrm{j}k_0 z'} \frac{\partial}{\partial r} G(r, z, z') \mathrm{d}z' \\
&= \hat{\boldsymbol{\varphi}} \frac{I_0}{2\pi r} \mathrm{e}^{-\mathrm{j}k_0 z} = \hat{\mathbf{z}} \times \frac{I_0 \mathbf{r}}{2\pi r^2} \mathrm{e}^{-\mathrm{j}k_0 z} = \hat{\mathbf{z}} \times \frac{1}{\eta_0} \mathbf{E}
\end{aligned}
\tag{14}
$$

To realize the direction of power flow, the complex Poynting vector (**S**) is calculated using the obtained electromagnetic fields,

$$
\mathbf{S} = \frac{1}{2} \mathbf{E} \times \mathbf{H}^* = \hat{\mathbf{z}} |I_0|^2 \frac{\eta_0}{2} \frac{1}{(2\pi r)^2} \tag{15}
$$

where star (*) denotes complex conjugate. This equation shows that the power flows only along z-axis and no power is radiated in radial direction. Also, the total power carried by the wave is shown to be infinity,

$$
P_{\text{Total}} = |I_0|^2 \frac{\eta_0}{2} \int_0^{\infty} \frac{1}{(2\pi r)^2} 2\pi r \mathrm{d}r = \infty \tag{16}
$$

2.2. Two Parallel Wires

In this case, two infinitely long and negligibly thin straight wires are positioned parallel to the z-axis at a distance d in a vacuum (Fig. 2). The wires are in the xz plane such that the first wire lies on the z-axis (i.e. $x = 0, y = 0$) while the second wire lies on the line $x = d$ and $y = 0$. The currents flowing through wire 1 and wire 2 are denoted as $I_1(z)$ and $I_2(z)$, respectively, and it is assumed

$$
I_1(z) = -I_2(z) = I_0 \mathrm{e}^{-\mathrm{j}k_0 z} \tag{17}
$$

Applying the superposition principle, the total electric and magnetic field intensities, **E** and **H** respectively, can be expressed as the sum of the fields produced by each individual wire:

$$
\mathbf{E}(\mathbf{R}) = \mathbf{E}_{\text{sw}}(\mathbf{R}) - \mathbf{E}_{\text{sw}}(\mathbf{R} - d\hat{\mathbf{x}}) \tag{18}
$$

$$
\mathbf{H}(\mathbf{R}) = \mathbf{H}_{\text{sw}}(\mathbf{R}) - \mathbf{H}_{\text{sw}}(\mathbf{R} - d\hat{\mathbf{x}}) \tag{19}
$$

where sw in subscript denotes single wire. In other words, $\mathbf{E}_{\text{sw}}$ and $\mathbf{H}_{\text{sw}}$ are, respectively, the electric and magnetic field intensities associated with single wire lying on z-axis. By substituting $\mathbf{E}_{\text{sw}}$ from (13), the electric field intensity of two parallel wires becomes

$$
\mathbf{E}(\mathbf{R}) = \frac{I_0 \eta_0}{2\pi} \frac{\mathbf{r}}{r^2} \mathrm{e}^{-\mathrm{j}k_0 z} - \frac{I_0 \eta_0}{2\pi} \frac{\mathbf{r} - d\hat{\mathbf{x}}}{|\mathbf{r} - d\hat{\mathbf{x}}|^2} \mathrm{e}^{-\mathrm{j}k_0 z} \tag{20}
$$

Expressing the vector **r** in Cartesian coordinates allows for further simplification of the electric field expression:

$$
\begin{aligned}
\mathbf{E}(\mathbf{R}) &= \frac{I_0 \eta_0}{2\pi} \left(\frac{\hat{\mathbf{x}} r \cos\varphi + \hat{\mathbf{y}} r \sin\varphi}{r^2} - \frac{\hat{\mathbf{x}}(r\cos\varphi - d) + \hat{\mathbf{y}} r \sin\varphi}{|\hat{\mathbf{x}}(r\cos\varphi - d) + \hat{\mathbf{y}} r \sin\varphi|^2} \right) \mathrm{e}^{-\mathrm{j}k_0 z} \\
&= \frac{I_0 \eta_0}{2\pi r} \left(\hat{\mathbf{x}} \cos\varphi + \hat{\mathbf{y}} \sin\varphi - \frac{\hat{\mathbf{x}}\left(\cos\varphi - \frac{d}{r}\right) + \hat{\mathbf{y}} \sin\varphi}{\left(\cos\varphi - \frac{d}{r}\right)^2 + \sin^2\varphi} \right) \mathrm{e}^{-\mathrm{j}k_0 z}
\end{aligned}
\tag{21}
$$

Defining the ratio d/r as δ, the previous equation can be simplified as follows

$$
\begin{aligned}
\mathbf{E}(\mathbf{R}) &= \frac{I_0 \eta_0}{2\pi r} \delta \left(\frac{\hat{\mathbf{x}}(\delta\cos\varphi - \cos 2\varphi) + \hat{\mathbf{y}}(\delta\sin\varphi - \sin 2\varphi)}{1 + \delta^2 - 2\delta\cos\varphi} \right) \mathrm{e}^{-\mathrm{j}k_0 z} \\
&= \frac{I_0 \eta_0}{2\pi r} \delta \left(\frac{\hat{\mathbf{r}}(\delta - \cos\varphi) - \hat{\boldsymbol{\varphi}} \sin\varphi}{1 + \delta^2 - 2\delta\cos\varphi} \right) \mathrm{e}^{-\mathrm{j}k_0 z}
\end{aligned}
\tag{22}
$$

Also, the corresponding magnetic field intensity with respect to the (14) and (22) is

$$
\begin{aligned}
\mathbf{H}(\mathbf{R}) &= \hat{\mathbf{z}} \times \frac{1}{\eta_0} \mathbf{E}(\mathbf{R}) \\
&= \frac{I_0}{2\pi r} \delta \left(\frac{\hat{\boldsymbol{\varphi}}(\delta - \cos\varphi) + \hat{\mathbf{r}} \sin\varphi}{1 + \delta^2 - 2\delta\cos\varphi} \right) \mathrm{e}^{-\mathrm{j}k_0 z}
\end{aligned}
\tag{23}
$$

Finally, the complex Poynting vector is

$$\mathbf{S}=\frac{1}{2}\mathbf{E}\times\mathbf{H}^{*}=\hat{\mathbf{z}}\left|I_0\right|^2\frac{\eta_0}{2}\left(\frac{\delta}{2\pi r}\right)^2\frac{1}{1+\delta^2-2\delta\cos\varphi} \quad (24)$$

3. SIMULATION

In this section, the radiation from a single infinitely long straight wire carrying a traveling-wave current $I_0\exp(-jk_0z)$ is analyzed using full-wave simulations in ANSYS HFSS [17]. As position-dependent current sources are not directly supported in this software, the continuous current distribution is approximated by discretizing the wire into electrically small segments. Each segment is excited by a uniform current source of 1A, with its phase assigned according to the axial position of the segment center to emulate the desired traveling-wave behavior.

The wire is enclosed within an air-filled cylindrical region whose lateral surface is terminated by a radiation boundary condition to represent an open environment. To emulate the infinite length of the wire, periodic (primary/secondary) boundary conditions are applied to the top and bottom faces of the domain.

The simulations are performed at 1GHz. To reduce computational complexity, only a finite section of length $\lambda_0/8$ is modeled. This section is discretized into 46 segments, where the first and last segments have a length of $\lambda_0/(8\times45\times2)$, and the remaining segments each have a length of $\lambda_0/(8\times45)$. The phase of each source is determined from the position of the corresponding segment center. In addition, the phase shift applied to the secondary boundary is set to-45deg, ensuring consistency with the imposed traveling-wave current distribution.

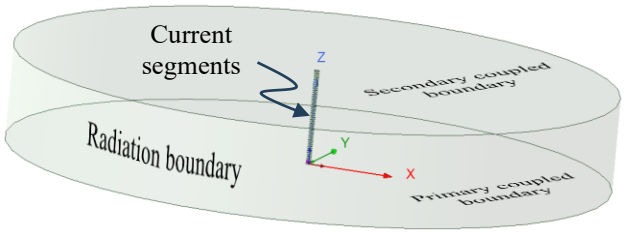


Fig. 3: Simulated structure in ANSYS HFSS.

The simulated field distributions are shown in Fig. 4. As observed, the electric field intensity is directed radially outward from the wire, while the magnetic field circulates around the wire, consistent with the expected transverse electromagnetic (TEM) behavior. Furthermore, the real part of the Poynting vector is predominantly aligned along the wire axis, indicating that the power flow is confined to the longitudinal direction with no radial radiation, in agreement with the analytical results.

The radial variation of the electric field is depicted in Fig. 5. The simulated results closely follow the r^{-1} trend predicted by the analytical formulation, confirming the inverse proportionality of the field magnitude with distance from the wire. This agreement further validates the accuracy of the analytical results derived in this work.

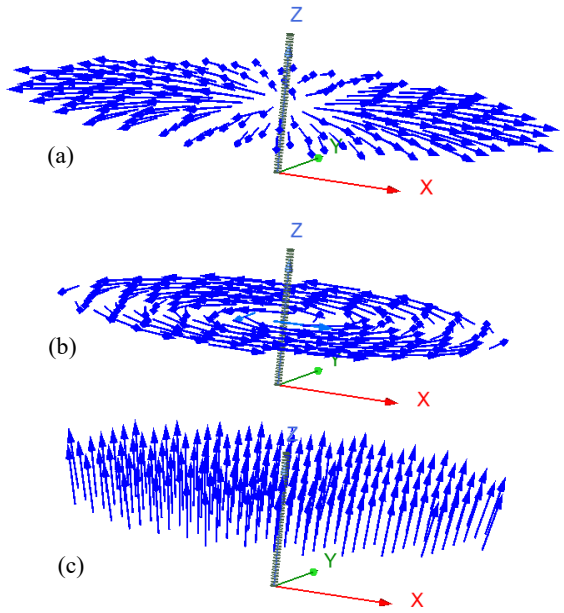


Fig. 4: Field distributions of the simulated structure: (a) electric field intensity vector, (b) magnetic field intensity vector, and (c) real part of the Poynting vector.

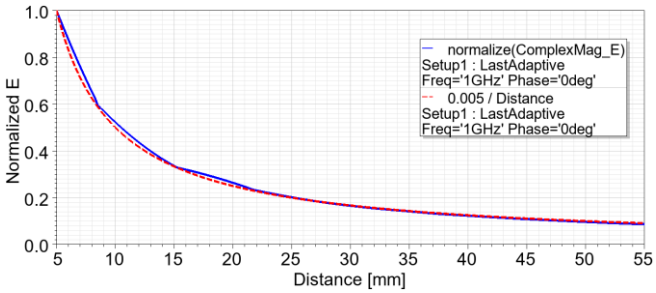


Fig. 5: Simulated normalized electric field magnitude as a function of radial distance (solid blue line), compared with the r^{-1} dependence (dashed red line).

4. DISCUSSION

In this section, the analytical results obtained are compared with established electromagnetic principles and existing literature to validate and interpret the findings.

For the single wire case, the absence of electric and magnetic field components along the z-axis confirms the presence of a Transverse Electromagnetic (TEM) wave. This characteristic ensures that power flow occurs solely along the wire, with no energy radiating outwards. The single straight wire can be conceptually viewed as a limiting case of a coaxial cable (Fig. 6) where the inner conductor radius approaches zero, and the outer conductor radius approaches infinity. The obtained electric and magnetic fields coincide with those of a coaxial cable [18], reinforcing the validity of our analysis. The characteristic impedance of a coaxial line is given by [18]

$$Z_c=\frac{\eta_0}{2\pi}\ln\left(\frac{b}{a}\right) \quad (25)$$

where a and b are the inner and outer conductor radii, respectively. In the limiting case of $a\to0$ and $b\to\infty$, $Z_c\to\infty$,

which aligns with the assumed finite current and infinite total power flow obtained in (16).

Turning to the two-wire scenario, the magnitude of the electric field intensity (22) tends toward infinity at the locations of the wires on the xy-plane, increasing with a rate proportional to r^{-1}. As a consequence, an infinite voltage emerges across the wires, leading to an infinite characteristic impedance. This is consistent with the behavior of a two-wire transmission line (Fig. 7), whose characteristic impedance is given by [1]

$$Z_c = \frac{\eta_0}{\pi}\cosh^{-1}\left(\frac{d}{2a}\right) \tag{26}$$

where a is the wire radius and d is the separation between the wires. In the limiting case of $a\to 0$, the impedance tends to infinity, thereby agreeing with the result obtained in our analysis.

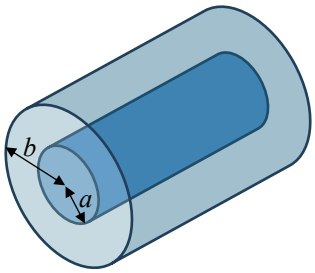


Fig. 6: Coaxial cable

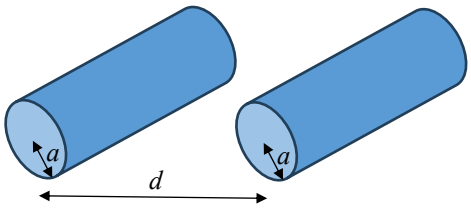


Fig. 7: Two wire transmission line

It is important to highlight that the consistent cross-sectional uniformity of the transmission line along its length contributes to maintaining a constant, real-valued characteristic impedance.

Similar to the case of a single wire, the absence of radiation perpendicular to the wire length in both scenarios stems from the transmission line's infinite length and the lossless nature of the transmission line and the surrounding medium.

It is important to note that while this paper focused on wires with zero radius, the presented methodology can be applied to analyze wires with volume or surface current distributions, provided the current density maintains the exp(-jk_0z) dependency along the z-axis, i.e.

$$\mathbf{J}(\mathbf{R}) = \mathbf{J}(r,\varphi,z) = \hat{\mathbf{z}}J_0(r,\varphi)\,\mathrm{e}^{-jk_0z} \tag{27}$$

In such cases, the absence of electric and magnetic field z-components would still hold for infinite length transmission lines, confirming the generality of the TEM wave propagation characteristic.

These findings contribute to a deeper understanding of electromagnetic wave behavior in ideal transmission line systems and serve as a steppingstone for exploring more complex and realistic configurations.

5. Conclusion

In this paper, the electric and magnetic field intensities for a single straight infinite-length wire and two parallel infinite-length wires have been analytically calculated. The absence of field components along the wire in both cases has been demonstrated, confirming that the radiated wave is TEM with respect to the radiation direction. To validate the analytical results, the single-wire configuration was simulated using a full-wave electromagnetic solver, and excellent agreement between the simulated and theoretical results was observed. Comparisons with the coaxial cable and two-wire problems with non-zero radius have also been conducted, further validating the obtained results.

This study has provided a clear understanding of the electromagnetic behavior in ideal transmission line systems. While the focus has been on lossless and infinitely long configurations, the presented methodology can be extended to analyze more complex scenarios involving wires with non-zero radius or specific current distributions. The misconception of radiation from infinitely long, lossless two-wire transmission lines has been dispelled, offering a solid theoretical foundation for future research and applications in the field of electromagnetics.

Acknowledgments

The author wishes to thank Prof. Fatih Dikmen of Gebze Technical University for his insightful discussions and valuable contributions to this work.

Declaration Of Competing Interest

The authors declare that they have no known competing financial interests or personal relationships that could have appeared to influence the work reported in this paper. The ethical issues; including plagiarism, informed consent, misconduct, data fabrication and/or falsification, double publication and/or submission, redundancy has been completely observed by the authors.

References

[1] D. K. Cheng, Field and wave electromagnetics, Pearson Education India, 1989.

[2] J. R. Carson, "Radiation from transmission lines," Journal of the American Institute of Electrical Engineers, vol. 40, no. 10, pp. 789–790, Oct. 1921.

[3] G. Mie, "Elektrische Wellen an zwei parallelen Drähten, " Annalen der Physik, vol. 2, pp. 201, 1900.

[4] H. M. Macdonald, Electric waves: being an Adams prize essay in the University of Cambridge. CUP Archive, 1902.

[5] C. P. Steinmetz, "The general equations of the electric circuit — III: Variation of constants R, L, C, and G, and its effects, " *Proceedings of the American Institute of Electrical Engineers*, vol. 38, no. 3, pp. 249-318, March 1919.

[6] C. Manneback, "Radiation from Transmission Lines," *Transactions of the American Institute of Electrical*

Engineers, vol. XLII, pp. 289-301, January-December 1923.

[7] G. Sinclair, "Theory of Models of Electromagnetic Systems," *Proceedings of the IRE*, vol. 36, no. 11, pp. 1364-1370, Nov. 1948.

[8] J. E. Storer and R. King, "Radiation Resistance of a Two-Wire Line," *Proceedings of the IRE*, vol. 39, no. 11, pp. 1408-1412, Nov. 1951.

[9] R. Ianconescu and V. Vulfin, "Radiation from free space TEM transmission lines," *IET Microwaves, Antennas & Propagation*, vol. 13, no. 13, pp. 2242-2255, July 2019.

[10] D. Tashiro, T. Hisakado, T. Matsushima and O. Wada, "Single-Conductor Transmission Line Model Incorporating Radiation Reaction," *IEEE Transactions on Electromagnetic Compatibility*, vol. 63, no. 4, pp. 1065-1077, Aug. 2021.

[11] W. Dai and P. G. Bremer, "Extended Resistance Matrix Formulation for Radiation Coupling of a Multi-Conductor Transmission Line," In *2024 IEEE International Symposium on Electromagnetic Compatibility, Signal & Power Integrity (EMC+ SIPI)*, pp. 558-558. IEEE, 2024.

[12] T. Liang, Z. Xi, T. Guo, Z. Wang, Y. Mu, B. Zhang, J. Guo, and Y.-Z. Xie, "Combining Baum–Liu–Tesche model and charge simulation method for analysis of electromagnetic field coupling to transmission lines inside underground utility tunnels," *IEEE Trans. Electromagn. Compat.*, vol. 67, no. 4, pp. 1282-1293, June 2025.

[13] D. Tashiro, K. Sameshima, T. Hisakado, A. M. Islam, and O. Wada, "Single-conductor transmission-line model for bent wire structures," IEEE Trans. Electromagn. Compat., vol. 65, no. 5, pp. 1432–1445, Oct. 2023.

[14] R. F. Harrington, "Sources of cylindrical waves," in *Time-Harmonic Electromagnetic Fields*, New York, NY, USA: Wiley, 2001, ch. 5, sec. 5-6.

[15] C. A. Balanis, "Radial waveguides," in *Balanis' Advanced Engineering Electromagnetics*, 3rd ed., Hoboken, NJ, USA: Wiley, 2024, ch. 9, sec. 9-4.

[16] C. A. Balanis, Antenna theory: analysis and design, John Wiley & Sons, 2016.

[17] ANSYS, Inc., *ANSYS Electronics Desktop 2024 R2*. Canonsburg, PA, USA: ANSYS, Inc., 2024.

[18] R. E. Collin, Foundations for microwave engineering, John Wiley & Sons, 2007.

Copyrights
© 2026 Licensee Shahid Chamran University of Ahvaz, Ahvaz, Iran. This article is an open-access article distributed under the terms and conditions of the Creative Commons Attribution –NonCommercial 4.0 International (CC BY-NC 4.0) License (http://creativecommons.org/licenses/by-nc/4.0/).